Plant Physiol. (1984) 74, 90–95
0032-0889/84/74/0090/06/$01.00/0

Influence of Iron Deprivation on the Membrane Composition of *Anacystis nidulans*[1]

Received for publication June 14, 1983 and in revised form September 25, 1983

JAMES A. GUIKEMA[2] AND LOUIS A. SHERMAN*
Division of Biological Sciences, University of Missouri, Columbia, Missouri 65211

ABSTRACT

Cultures of the cyanobacterium *Anacystis nidulans* were grown under iron-deficient conditions and then restored by the addition of iron. Membrane proteins from iron-deficient and iron-restored cells were analyzed by lithium dodecyl sulfate-polyacrylamide gradient gel electrophoresis. The incorporation of [^{35}S]sulfate into membrane proteins and lactoperoxidase-catalyzed ^{125}I iodination were used to monitor the rates of polypeptide biosynthesis and surface exposure of membrane proteins, respectively. These polypeptide profiles revealed major differences in the membrane composition of iron-deficient and normal cells. Iron deficiency caused a decrease in the amount of certain important membrane proteins, reflecting a decreased rate of biosynthesis of these peptides. Several photosystem II peptides also showed an increase in surface exposure after iron stress. In addition, iron deficiency led to the synthesis of proteins at 34 and 52 kilodaltons which were not present in normal cells. When iron was restored to a deficient culture, a metabolic sequence was initiated within the first 12 h after the addition of iron which led to phenotypically normal cells. Pulse labeling with [^{35}S]sulfate during this period demonstrated that iron addition initiates a coordinated pattern of synthesis that leads to the assembly of normal membranes.

The thylakoid membranes of cyanobacteria show changes in response to iron deprivation (8, 17–19). We have previously documented the major changes in the light-harvesting system of *Anacystis nidulans* that occurred during low iron growth (8). Cells deprived of iron contained lowered amounts of Chl *a* and of phycocyanin, indicating a lowered rate of pigment biosynthesis. Our data suggested that iron deficiency disrupted the light-harvesting matrix of cyanobacterial thylakoids by altering the composition of these membranes. For example, the light-harvesting efficiency for PSI was decreased, and the patterns of Chl fluorescence were altered both at room temperature and at 77 K. Fluorescence kinetics monitored at room temperature showed an increase in fluorescence yield and a decrease in the extent of variable fluorescence. The Chl fluorescence emission spectrum at 77 K was altered as well. Three emission peaks, at 686, 696, and 716 nm, are characteristic of *A. nidulans* fluorescence at this temperature. Iron deficiency caused a reduction in fluorescence emission at 696 and 716 nm, and a corresponding increase at 686 nm. These changes in the biophysical parameters spurred an examination of the Chl-protein arrangement of iron-deficient thylakoids. We observed a loss of the large mol wt Chl-protein complexes normally associated with these membranes (5, 7). Furthermore, we suggested that, by monitoring membrane synthesis following the readdition of iron, we would be able to detect peptides responsible for the altered membrane structure.

We have analyzed polypeptide patterns by gel electrophoresis to document the alterations in thylakoid protein composition caused by iron deficiency in *A. nidulans*. Certain peptides are accumulated in the membrane fraction upon iron stress, while others are lost. Membranes from iron-stressed cells show a different topology, as monitored by the lactoperoxidase-catalyzed iodination of surface-exposed tyrosines. *In vivo* incorporation of [^{35}S]sulfate into protein was used as a monitor of peptide synthesis during both iron stress and the recovery from iron deficiency. Maximum changes in photosynthetic parameters occurred during the first 7 to 13 h following the addition of iron to a deficient culture. These changes lead to the addition of membrane proteins which are important for normal photosynthetic membrane structure.

MATERIALS AND METHODS

Cells of *A. nidulans* R2 were obtained and grown in shaking culture as previously described (8). Optimal growth was obtained using BG-11 growth medium. Iron-deficient media was prepared by replacing ferric ammonium citrate with equal molar amounts of ammonium citrate in this medium. Glassware was rinsed thoroughly with glass-distilled H_2O prior to use. The effects of iron deficiency were observed 3 to 5 d following inoculation. In the experiments described here, deficient cultures were inoculated from cultures which were themselves iron deficient. Unless otherwise noted, membranes were prepared from normal and iron-deficient cultures by lysozyme treatment of cells, followed by osmotic rupture and differential centrifugation (5). Membranes were suspended and stored at −70°C in 20 mM Tricine, 0.5 M mannitol, 5 mM $NaKHPO_4$, pH 7.5. Toluenesulfonyl fluoride (20 μg/ml) was added throughout the membrane isolation protocol to inhibit protease activity.

The fraction shown in Figure 3A was isolated as follows. Cells were harvested by centrifugation and resuspended in 10 mM Tricine (pH 7.5) containing protease inhibitors (toluenesulfonyl fluoride, 20 μg/ml; norleucine, 1 mM; benzamadine, 1 mM), and then frozen at −20°C. Cells were then thawed, sonicated in an ice bath with two pulses of 2 min each, and unbroken cells were removed by centrifugation. A 3-min spin (12,000*g*) in an Eppendorf microfuge pelleted a dense fraction, containing almost no Chl. A green supernatant remained, containing most of the thylakoids and soluble membranes. The pellet was washed twice in buffer and solubilized for electrophoresis.

Membrane proteins were labeled with ^{35}S by resuspending logarithmically growing cells in growth medium (either BG-11

[1] Supported by National Institutes of Health grant GM21827, an N. I. H. Postdoctoral Fellowship (GM07704) to J. A. G., and by the University of Missouri Institutional Biomedical Research Grant RR07053 from N. I. H. This report represents contribution number 84-79J of the Kansas Agricultural Experiment Station.

[2] Present address: Division of Biology, Kansas State University, Manhattan, KS 66506.

or iron-deficient BG-11) that contained one-tenth the normal concentration of sulfate. $Na_2{}^{35}SO_4$ was added to a concentration of 10 to 50 μCi/ml, and cultures were labeled for 2 h in the light (6). Cells were harvested and membranes prepared as described above. These procedures typically yielded labeled membranes containing 5,000 to 10,000 cpm/μg membrane protein. Lactoperoxidase-catalyzed iodination of surface-exposed amino acids in membrane proteins was performed as described previously (6). Under the conditions employed, omission of lactoperoxidase resulted in less than 1% of the iodination achieved in the presence of the enzyme. Typically, ^{125}I incorporation occurred to 1,000 to 5,000 cpm/μg membrane protein.

Acrylamide gel analysis of membrane protein composition was achieved using a modification (6) of the LDS[3] procedure of Delepelaire and Chua (2). Membranes (4 mg protein/ml) were solubilized in 2% LDS, 10 mM Tricine, 5% β-mercaptoethanol (pH 7.5) for 15 min at 70°C, and electrophoresis was performed at 4°C. Gels were stained with Coomassie Brilliant Blue R-250, photographed using Kodak 2415 film, and dried onto filter paper. Autoradiographic profiles were developed by exposing dried gels to Kodak X-Omat AR-5 film (1–7 d). In each electrophoretic experiment, gels were layered with sample in two ways: (a) by layering constant amounts of protein (80 μg protein/well); and (b) by adding constant amounts of radioactivity. The staining pattern and autoradiographic profiles were examined visually. In each profile shown here (except Fig. 3A), membrane peptides are identified by the band numbering system devised earlier (6). This system will allow a comparison of our results here with the data which we used in formulating a topological model of *A. nidulans* thylakoids (6, 7).

Fluorescence at 77 K was monitored using an Aminco Bowman spectrofluorimeter modified with a Hamamatsu R666S photomultiplier tube (16). Cells were frozen in 60% glycerol to minimize crystal fracture formation. Light absorption was measured using an Aminco DW-2 spectrophotometer, and Chl:phycocyanin ratios were estimated using the equations of Jones and Myers (10).

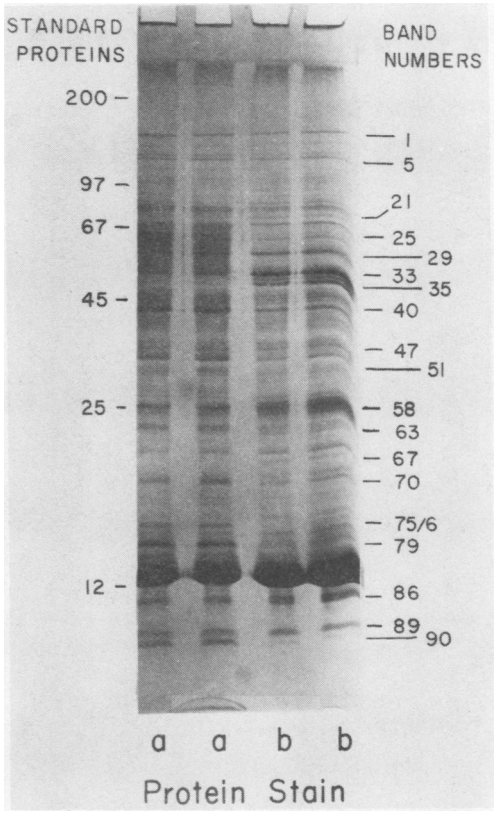

FIG. 1. Electrophoretic profile showing the Coomassie Blue R staining patterns of membrane proteins of normal (lane a) and iron-deficient (lane b) cells of *A. nidulans*. Solubilized membranes (50–80 μg of protein) were layered on a 10 to 20% polyacrylamide gradient gel, and were run overnight at 2.5 w of constant power. Standard proteins served as markers to estimate the migration patterns based on mol wt, and polypeptide bands were numbered in accordance with a system devised earlier (6).

RESULTS

Membrane Composition and Topology. Figure 1 demonstrates the influence of iron deficiency on the protein composition of *A. nidulans* thylakoids. Polypeptide profiles were obtained on a LDS polyacrylamide gradient gel, and thylakoid proteins from normal cells (lane a) and iron-deficient cells (lane b) were compared. Polypeptide bands were numbered with the system we devised earlier to present a topological model of these membranes (6).

An examination of Figure 1 indicated that each polypeptide band could be assigned to one of three classes. First, several peptides were present in roughly similar amounts in both normal and iron-deficient membrane preparations. The peptides at bands 1 and 5 were two of many examples. These proteins were not influenced by iron-limited growth and, therefore, were used as markers when comparing patterns of different membrane preparations. Second, a few polypeptides were enhanced by iron deficiency. For example, increased staining was evident at bands 21, 22, 33, 34, 35, 57–59, 63, 67, 73, and 86. In addition, iron deficiency generated a new peptide at band 48/49; although this protein is not prominent in Figure 1, it will be demonstrated convincingly below.

The third and largest class of polypeptide bands were those present in reduced amounts after iron-deficient growth. These included peptides at bands 25, 27, 28, 30–32, 36, 38, 40, 49, 51, 55, 61, 62, 64, 71–73, 75, 76, 79, and 90. This class accounted for most of the differences between the two types of membrane preparations, and is consistent with the suggestion that either protein biosynthesis or assembly is modified during iron deficiency (12, 20).

Certain regions of Figure 1 merit a more careful examination. For example, several minor bands between 55 and 70 kD diminished during iron-deficient growth. In contrast, the major bands in this region either remained constant (*e.g.* bands 26 and 29) or were increased (such as bands 33–35). It is possible that several of the minor bands represented partial digestion products of band 25, which we believe is the Chl-binding protein associated with PSI (6). A second interesting region in the profiles of Figure 1 concerned bands 61–63. These peptides often appeared as a closely spaced triplet on this gel system. Iron deficiency caused an increase in band 63, seemingly at the expense of the two larger peptides. This type of relationship was observed among other doublets and triplets as well.

Figure 1 shows that iron deficiency produced an aberrant membrane polypeptide composition. It seemed likely that topological alterations would accompany these changes in composition. Figure 2 presents an experiment to monitor membrane topology by labeling surface-exposed polypeptides and compares the lactoperoxidase ^{125}I iodination patterns of normal (lanes b and c) and iron-deficient (lanes d and e) membranes. Lane a presents a ^{35}S-labeled polypeptide profile for comparison. Lanes (b + c) and (d + e) of Figure 2 can be directly compared to lanes a and b of Figure 1, respectively.

The iodination patterns in Figure 2 demonstrated numerous differences in protein topology between normal and iron-deficient membranes. For many peptide bands, iron deficiency re-

[3] Abbreviation: LDS, lithium dodecyl sulfate.

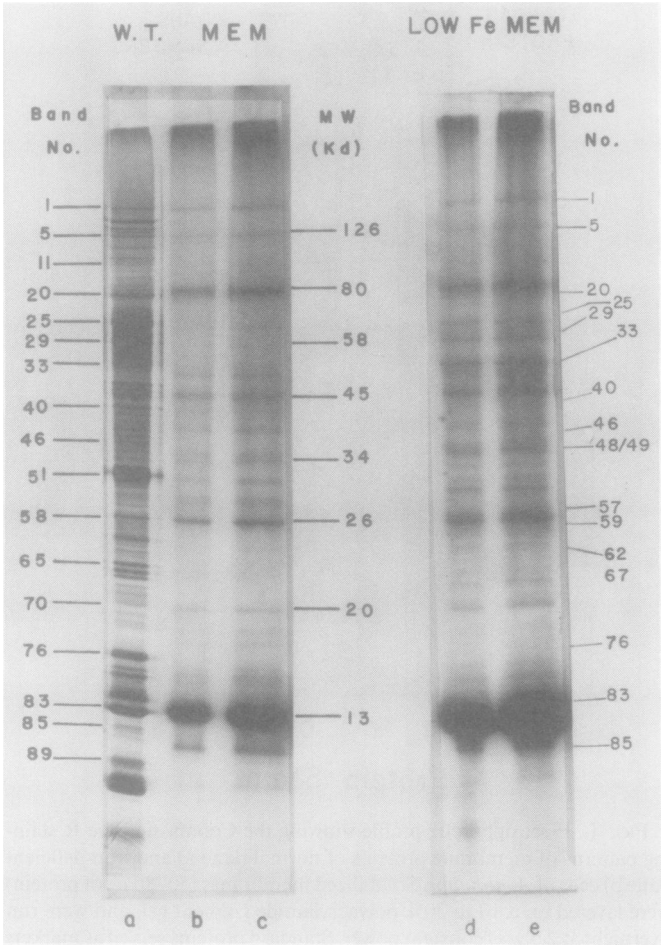

FIG. 2. Electrophoretic profile showing ^{125}I iodination patterns of membrane proteins from normal (lanes b and c) and iron-deficient (lanes d and e) cells of *A. nidulans*. For comparison, lane a shows a ^{35}S-labeled pattern of membrane proteins from normal cells. Isolated membranes were labeled using lactoperoxidase-catalyzed ^{125}I iodination as a surface probe. A constant amount of radioactivity (250,000 cpm) was layered in each well, corresponding to 50 to 80 μg of protein/well.

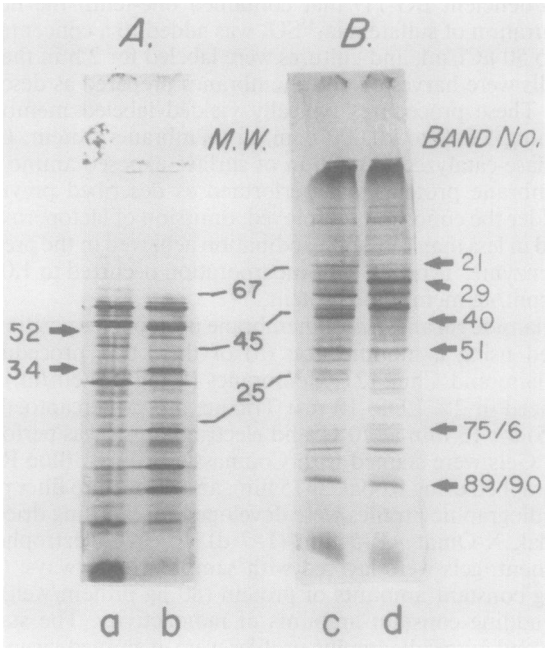

FIG. 3. Electrophoretic profiles showing [^{35}S]sulfate incorporation into a dense fraction (A) and a thylakoid membrane fraction (B) of normal (lanes a and c) and iron-deficient (lanes b and d) cells. The isolation of the fractions is described in "Materials and Methods." A constant amount of radioactivity was added to lanes a and b (275,000 cpm/well) and to lanes c and d (375,000 cpm/well).

sulted in an increased labeling, as was observed for bands 4, 20, 21, 25, 26, 29, 33, 34, 35, 46, 47, 50, 53, 57, 59, 60, 62, 63, and 67. For a majority of these bands, increased labeling occurred despite a loss in bulk protein as seen in Figure 1. Only at seven band positions (bands 21, 33–35, 57, 59, and 63) did increased iodination correspond to an increase in protein content, as monitored in Figure 1. For the remainder, increased surface labeling possibly reflected a loss in the shielding of the protein from the aqueous membrane surface. A major ^{125}I-labeled band was observed in Figure 2 at band 48/49 in iron-deficient cells. We believe that this diffuse band represents two proteins of approximately 34 kD. One of the proteins is present in normal membranes and becomes more exposed in low iron membranes. The second species has many surface-exposed sites, and may not be a component of the photosynthetic membrane.

The new band at 34 kD was similar in size to proteins which are important in photosynthesis. For example, cyanobacterial Cyt *f* has an electrophoretic mobility of 33 kD when completely denatured in LDS (5). Figure 3A represents a ^{35}S autoradiographc profile of a fraction which was enriched in the novel 34 kD protein. A peptide at 52 kD also appeared in response to iron deficiency. Although three other proteins with mol wt under 25 kD showed greatly increased incorporation, only the 34 and 52 kD species represented synthesis of new proteins induced by iron-deficient growth. The fraction enriched in these two proteins contained little Chl, and pelleted prior to a thylakoid membrane fraction under the conditions described in Figure 3; this suggested a different origin for the 34 kD peptide. One possibility is that the 34 and 52 kD peptides were outer membrane proteins which functioned in binding Fe-containing siderophores (1, 15, 23). This would explain their induction by iron-deficient conditions, a strong labeling with surface probes, and the pelleting with a fraction heavier than thylakoid membranes.

Biosynthetic Incorporation of Label into Membrane Proteins. The altered patterns of membrane composition and topology depicted in Figures 1 and 2 could have arisen in several ways. These include decreased protein synthesis, aberrant membrane assembly, and an increased turnover of specific membrane polypeptides. To discriminate among these possibilities, we initiated experiments to monitor the *in vivo* incorporation of [^{35}S]sulfate into membrane proteins. Radiolabel incorporation during iron deficiency occurred at a rate approximately 75% of that found in normal cells, indicating that these cells were still metabolically active. Therefore, electrophoretic assessment of these membrane fractions should show if specific peptides were being actively synthesized during iron deficiency.

Figures 3B and 4 (lanes a and b) present two experiments which compared the peptide biosynthesis of normal and iron-deficient cells. Several major differences in polypeptide biosynthesis accompanied iron deficiency, and notable examples in Figure 3B are highlighted by arrows. A peptide at 78 kD showed an enhanced radiolabel incorporation in iron-deficient cells, despite a net decrease in peptide staining at this position. Alternatively, several polypeptide bands showed a decrease in synthesis. The proteins at 14, 21, and 33 kD were especially interesting because their mol wt were similar to the photosynthetic Cyt in *A. nidulans* (5). These findings suggested that changes in membrane composition resulted from both diminished synthesis of certain peptides (or enhanced breakdown of these species), plus

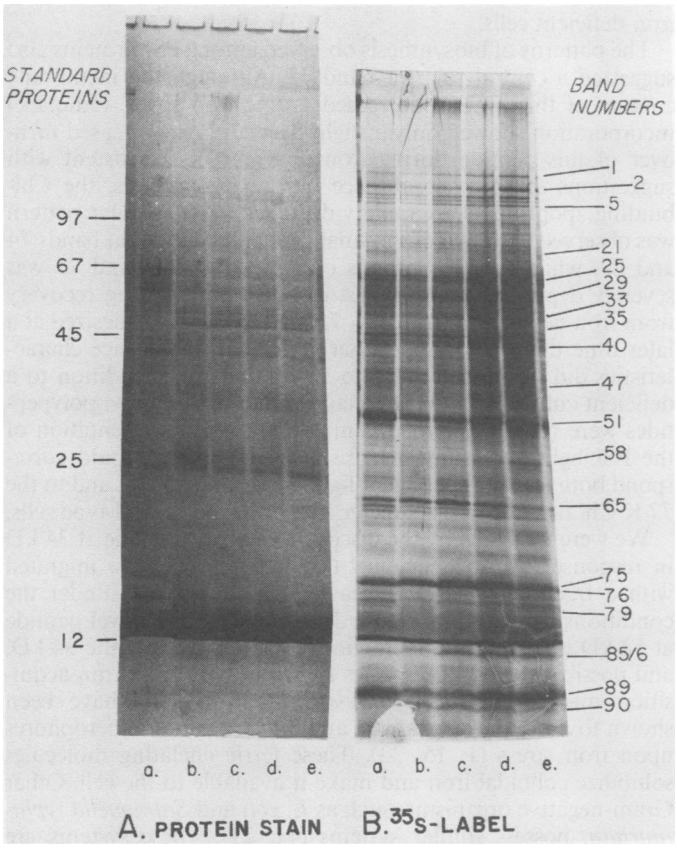

FIG. 4. ^{35}S incorporation into membrane proteins at different times after iron restoration to an iron-deprived culture of *A. nidulans*. Both the Coomassie Blue R staining pattern (A) and the autoradiographic profile of ^{35}S incorporation (B) are shown. Cells from normal (lane a) and iron-deficient (lane b) cultures were labeled with [^{35}S]sulfate for 2 h in the light. Ferric ammonium citrate was added to the iron-deficient culture, and those cells were incubated with [^{35}S]sulfate 0 to 2 h (lane c), 3 to 5 h (lane d), and 7 to 9 h (lane e) after the addition of iron. Constant amounts of protein (80 μg protein/well) were added to each lane, resulting in a range of radioactivity (from 210,000 to 310,000 cpm/well).

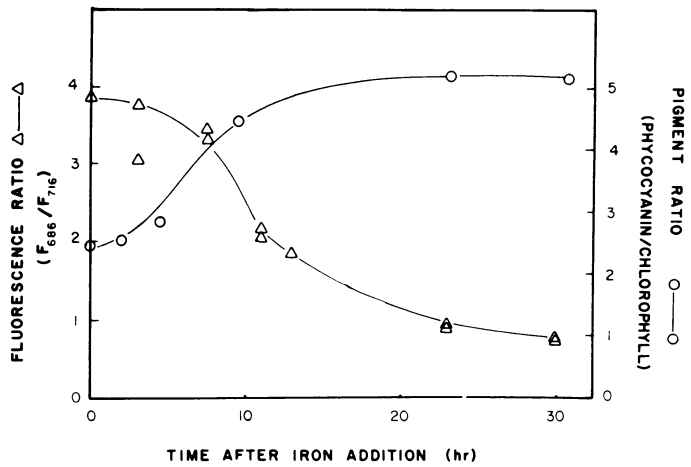

FIG. 5. Effects of iron addition on the Chl fluorescence characteristics and pigment composition of iron-deficient *A. nidulans*. Ferric ammonium citrate (25 μM) was added to an iron-deficient culture. The pigment composition (10) and 77 K Chl fluorescence spectra (16) of these cells were monitored, and the results were calculated as a ratio of Chl to phycocyanin and a ratio of the fluorescence peak heights at 686 and 716 nm.

enhanced synthesis of others. To extend our studies, we chose to examine the polypeptide profiles of cyanobacterial thylakoids at differing stages in recovery from iron deficiency.

Recovery of Cyanobacteria from Iron Deficiency. Figure 5 shows the effects of iron readdition on Chl fluorescence of an iron-deficient culture. Chl fluorescence at 77 K was the most sensitive indicator for membrane stress. Emission at 696 and 716 nm was severely depressed in iron-deficient cells. However, when iron was reintroduced to a deficient culture, the ratios of F686:F696 and F686:F716 decreased and the phycocyanin-to-Chl ratio increased with similar kinetics. Recovery from iron stress began approximately 4 to 6 h after addition of iron and was virtually completed by 12 to 14 h (Fig. 5). Therefore, we focused on the time period prior to 12 h after iron addition in our analysis of membrane protein synthesis during reconstitution.

Polypeptide profiles of membranes isolated at different times following the readdition of iron to a stressed culture are shown in Figure 4. Each sample was labeled for 2 h prior to membrane isolation, and the electrophoretic conditions were identical to those in Figures 1 and 2. Figure 4 shows the Coomassie Blue staining (A) and the corresponding autoradiogram (B) of samples that were taken: from cells growing in complete medium (lane a); from cells growing in iron-deficient medium (lane b); or 2 h (lane c), 5 h (lane d), and 9 h (lane e) after the addition of iron to iron-deficient cells.

Figure 4 reinforced the results on iron-deficient membrane proteins discussed in Figures 1 and 3, and also demonstrated numerous changes in protein synthesis during reconstitution. These results are summarized in Table I, and are presented in the context of the known structural and functional relationships in *A. nidulans* thylakoids (6). Three classes of peptides are represented: (a) PSI peptides, incuding those observed in PSI particles and in PSI-associated Chl-proteins; (b) PSI peptides, obtained from data similar to the above; and (c) iron-containing peptides, including those with heme and presumptive iron-sulfur ligands. Table I also summarizes the topological information presented in Figure 2. The data indicate that synthesis of most of these membrane proteins began by 3 h after iron addition, which was consistent with the physiological data (*e.g.* Fig. 5). There were a few exceptions (bands 21, 47, and 79) that did not begin synthesis until 7 h after iron addition. The data imply that membrane protein synthesis is coordinately regulated after the addition of iron.

DISCUSSION

In this report, we have presented a detailed look at the composition, topology, and synthesis of membrane polypeptides in iron-deficient cells of *A. nidulans*. The context of our presentation is an interest in the photosynthetic physiology of this organism and, as detailed in prior reports (8, 17–19), iron-deficient cells are markedly different in certain photosynthetic parameters. Nonetheless, iron-deficient cells are functional and grow normally. Based upon site-specific polypeptide labeling (22), detergent fractionation studies (7, 16), analyses of photosynthetic mutants (22), and polypeptide profiles, we have formulated a model of the composition and topology of *A. nidulans* thylakoids. Our model predicts a relationshp between certain photosynthetic parameters (such as Chl fluorescence at 77 K) and specific membrane proteins. The characteristics of iron-deficient cells provide an opportunity to examine our model within the context of altered membranes.

Changes in Chl fluorescence suggest that Chl has an altered environment in iron-deficient cells. As originally observed by Oquist (19), iron deficiency diminishes certain emission peaks when Chl fluorescence is monitored at 77 K. Emission at 716

Table I. *Effects of Iron Starvation and Recovery on the Membrane Proteins of Anacystis nidulans*

The effects of iron starvation are summarized by comparing the membrane polypeptide profiles from iron-deficient cells with profiles of normal cells. For each peptide band, changes in bulk protein content (Stain), the level of ^{35}S incorporation (^{35}S label), and the extent of surface exposure (^{125}I label) are expressed as: 0, no change; −, decreased; +, increased; and NL, not labeled. In addition, the time at which synthesis of the protein during recovery from iron deficiency is noted (Time of Recovery).

Band No.	Protein Content		^{125}I Label	Time of Recovery
	Stain	^{35}S label		
				h
PSI peptides				
PSI particles and CP I				
25	−	−	+	2
75	−	−−−	NL	5
89	0	−	0	2
PSI particles alone				
67/8	ND	−	++	5
85	ND	−	+	2
CP I alone				
74	−	−	0	5
79	−	−	0	9
90	−	+	NL	2
^{59}Fe-labeled peptides				
64	−	−	−	2
PSII peptides				
PSII particles and CP VI				
36	−	−	0	2
38	−	−	0	2
PSII particles alone				
21	+	−	+	9
40	−	−	−	2
47	0	−	++	9
51	−	0	−	2
72	−	−	NL	5
73	−	−	0	5
Heme-containing peptides				
49	−	−	NL	5
71	−	−	NL	5

and 696 nm is depressed and there is a corresponding rise in emission at 686 nm. This is illustrated in Figure 5 by presenting the changes in the ratio of 686 to 716 nm fluorescence emission during restoration from iron stress. Two other monitors suggest an altered environment for Chl: the red absorption peak for Chl is shifted (from 678 to 673 nm), and the Chl fluorescence yield at room temperature is dramatically increased.

The aberrant spectral parameters observed after iron deprivation may be explained by alterations in membrane organization. Iron-deficient cells have an altered Chl-protein composition (8, 13). Furthermore, electrophoresis of *A. nidulans* membranes revealed Chl-protein aggregates which contained many peptides also found in PSI preparations (7). Band 25 was considered as the major PSI Chl-binding protein, and several smaller peptides reproducibly associated with band 25 in Chl-protein aggregates (*e.g.* bands 74, 75, 79, and 89). Iron-deficient cells lack these Chl-protein aggregates (8), and also have a diminished content of the smaller peptides observed in the aggregates (Table I). Perhaps these smaller peptides function (at least in part) to orient PSI within the matrix of the membrane and, thereby, to maximize excitation transfer from the Chl antennae molecules to the PSI reaction center. An accurate measure of the Chl antennae pool with respect to the number of reaction centers is needed for iron-deficient cells.

The patterns of biosynthesis observed among PSI proteins also suggested a central role for band 25. Although the membrane content of this protein decreased during iron stress, radiolabel incorporation showed only a slight decrease. An increased turnover of this peptide during iron deficiency is consistent with suggestions that, in the absence of Chl biosynthesis, the Chl-binding apoproteins are rapidly degraded (9). A similar pattern was observed with two of the small PSI polypeptides at bands 74 and 89, while the biosynthesis of the peptide at band 75 was severely depressed upon iron stress. However, during recovery from iron deficiency, bands 74, 75, and 89 were synthesized at a later time than band 25. Similarly, normal fluorecence characteristics did not arise until 7 to 13 h after iron readdition to a deficient culture (Fig. 5). If certain of the small mol wt polypeptides were responsible for maintaining a normal orientation of the PSI light-harvesting matrix, their resynthesis would correspond both to a more efficient light harvesting for PSI and to the 77 K Chl fluorescence characteristics observed in wild-type cells.

We were intrigued by the discovery of a new peptide at 34 kD in response to iron deficiency (Fig. 3). This peptide migrated with a fraction which was heavier than thylakoids under the conditions described in Figure 3A. In addition, a novel peptide at 52 kD was seen in this fraction. It is possible that the 34 kD, and possibly the 52 kD, species represent part of an iron acquisition mechanism in *A. nidulans*. Cyanobacteria have been shown to excrete hydroxamate and dihydroxamate siderophores upon iron stress (1, 15, 23). These ferric chelating molecules solubilize colloidal iron and make it available to the cell. Other Gram-negative organisms, such as *E. coli* and *Salmonella typhimurium*, possess similar systems (11, 21). These systems are controlled, in part, by an induction of outer membrane proteins (11). Peptides in the 33 to 36 kD range are induced in these organisms, and these peptides serve to recognize and bind siderophore-iron chelates. It is possible that the novel 34 kD peptide observed here represents such a 'porin' protein. We are currently continuing the isolation of an outer membrane fraction to more carefully examine this possibility.

The major utility of these findings concerns the membrane biosynthesis which accompanies recovery from iron deficiency. *A. nidulans* is largely photoautotrophic, and experiments such as greening studies in chloroplasts (9) are not possible. This is unfortunate, since the prokaryotic nature of this organism makes it ideal for use in studying thylakoid biogenesis. Using this prokaryote, we can avoid the complex interplay between chloroplastic and nuclear genomes, and can focus on the mechanism of protein assembly. Our preliminary results, we believe, indicate a stepwise assembly of the photosynthetic apparatus. Chl-binding proteins appear first, and proteins which surround the core of these submembrane structures appear later. This later peptide synthesis coincides with alterations in Chl fluorescence which suggests that these peptides play a role in directing energy transfer during light harvesting.

Several recent reports suggest a stepwise assembly process for thylakoids of chloroplasts (9). Ohad and colleagues (4), using the y-1 mutant of *Chlamydomonas reinhardtii* studied light-activated greening in the presence of protein synthesis inhibitors. By comparing 77 K Chl fluorescence spectra, electron transport activity, and peptide synthesis, they were able to distinguish a sequence of developmental states during membrane biogenesis. Biosynthesis of peptides comprising reaction centers of PSI and PSII correlated with emerging electron transport activities. Synthesis of one peptide at 68 kD and two peptides between 20 and 35 kD was linked with formation of Chl-protein complexes which serve as intermediate antennae, thus increasing quantum yield. They ascribe the 686 nm fluorescence emission to Chl associated with a light-harvesting complex for PSII. Similarly, Arntzen and

coworkers (14), using barley and cucumber, observed a sequential synthesis of PSI. Chloroplasts greened using intermittent light lacked polypeptides in the 21.5 to 24.5 kD range and were deficient in 77 K fluorescence emission at 736 nm.

Similarly, our preliminary results on membrane synthesis during recovery from iron deficiency link polypeptides at bands 75 and 79 with a recovery of specific 77 K Chl fluorescence emission peaks. Because photosynthetic electron transport is not severely inhibited by limiting iron, bands 75 and 79 must not play an essential role in functions of PSI. Rather, the role of these peptides probably lies in the association of PSI with a light-harvesting matrix of the membrane and their low concentration in iron-deficient cells is probably coupled to the altered light-harvesting efficiency observed in these cells.

LITERATURE CITED

1. ARMSTRONG JE, C VAN BAALEN 1979 Iron transport in microalgae: The isolation and biological activity of a hydroxamate siderophore from the blue-green alga, *Agmenellum quadruplicatum*. J Gen Microbiol 111: 253–262
2. DELEPELAIRE P, N-H CHUA 1979 Lithium dodecyl sulfate polyacrylamide gel electrophoresis of thylakoid membranes at 4 C: Characterization of two additional chlorophyll a-protein complexes. Proc Natl Acad Sci USA 76: 111–115
3. GANTT E 1981 Phycobilisomes. Annu Rev Plant Physiol 15: 883–889
4. GERSHONI JM, S SHOCAT, S MALKIN, I OHAD 1982 Functional organization of the chlorophyll-containing complexes of *Chlamydomonas reinhardtii*. Plant Physiol 70: 637–644
5. GUIKEMA JA, LA SHERMAN 1981 Electrophoretic profiles of cyanobacterial membrane peptides showing heme-dependent peroxidase activity. Biochim Biophys Acta 637: 189–201
6. GUIKEMA JA, LA SHERMAN 1982 Protein composition and architecture of the photosynthetic membranes from the cyanobacterium, *Anacystis nidulans*. Biochim Biophys Acta 681: 440–450
7. GUIKEMA JA, LA SHERMAN 1983 Chlorophyll-protein organization of membranes from the cyanobacterium *Anacystis nidulans*. Arch Biochem Biophys 220: 155–166
8. GUIKEMA JA, LA SHERMAN 1983 Organization and function of chlorophyll in membranes of cyanobacteria during iron starvation. Plant Physiol 73: 250–256
9. HERRMANN FG, T BORNER, R HAGEMANN 1980 Biogenesis of thylakoids and the membrane-bound enzyme systems of photosynthesis. *In* J Reinert, ed, Chloroplasts, Results and Problems in Cell Differentiation, Vol 10. Springer-Verlag, New York, pp 149–177
10. JONES LW, J MYERS 1965 Pigment variations in *Anacystis nidulans* induced by light of selected wavelengths. J Phycol 1: 7–14
11. KADNER FJ, K HELLER, JW COULTON, V BRAUN 1980 Genetic control of hydroxamate-mediated iron uptake in *Escherichia coli*. J Bacteriol 143: 256–264
12. LAULHERE JP, R MACHE 1978 Induction des syntheses de mRNA et rRNA chloroplastique par le fer lors du verdissement de feulles chlorosees. Physiol Veg 16: 643–656
13. MACHOLD O 1971 Lamellar proteins of green and chlorotic chloroplasts affected by iron deficiency and antibiotics. Biochim Biophys Acta 238: 324–331
14. MULLETT JE, JJ BURKE, CJ ARNTZEN 1980 A developmental study of photosystem I peripheral chlorophyll proteins. Plant Physiol 65: 823–827
15. MURPHY TO, DR LEAN, C NALEWAJKO 1976 Blue-green algae: Their excretion of iron selective chelators enables them to dominate other algae. Science 192: 900–902
16. NEWMAN PJ, LA SHERMAN 1978 Isolation and characterization of photosystem I and II membrane particles from the blue-green alga, *Synechococcus cedrorum*. Biochim Biophys Acta 503: 343–361
17. OQUIST G 1971 Changes in pigment composition and photosynthesis induced by iron deficiency in the blue-green alga, *Anacystis nidulans*. Physiol Plant 25: 188–191
18. OQUIST G 1974 Iron deficiency in the blue-green alga, *Anacystis nidulans*: Changes in pigmentation and photosynthesis. Physiol Plant 30: 30–37
19. OQUIST G 1974 Iron deficiency in the blue-green alga, *Anacystis nidulans*: Fluorescence and absorption spectra recorded at 77 K. Physiol Plant 31: 55–58
20. PRICE CA 1968 Iron compounds and plant nutrition. Annu Rev Plant Physiol 19: 239–248
21. ROSENBERG H, IG YOUNG 1974 Iron transport in the enteric bacteria. *In* JB Neilands, ed, Microbial Iron Metabolism, Academic Press, New York, pp 1–250
22. SADEWASSER DA, LA SHERMAN 1981 Internal and external membrane proteins of the cyanobacterium, *Synechococcus cedrorum*. Biochim Biophys Acta 640: 326–340
23. SIMPSON FB, JB NEILANDS 1976 Siderochromes in Cyanophyceae: Isolation and characterization of schizokinen from *Anabaena*. J Phycol 12: 44–48